Journal of Alloys and Compounds 509 (2011) 3771–3776

Contents lists available at ScienceDirect

Journal of Alloys and Compounds

journal homepage: www.elsevier.com/locate/jallcom

Facile hydrothermal synthesis and characteristics of B-doped TiO_2 hybrid hollow microspheres with higher photo-catalytic activity

Jian Zheng[a,b], Zhongqing Liu[b,*], Xu Liu[b], Xin Yan[b], Dandan Li[b], Wei Chu[a,b,*]

[a] Key Laboratory of Green Chemistry and Technology of Ministry of Education, Department of Chemistry, Sichuan University, Chengdu 610064, China
[b] Department of Chemical Engineering, Sichuan University, Chengdu 610065, China

ARTICLE INFO

Article history:
Received 9 October 2010
Received in revised form
15 December 2010
Accepted 20 December 2010
Available online 28 December 2010

Keywords:
Hybrid hollow microspheres
Doped titanium dioxide
Boron additive
Hydrothermal synthesis
Photo-catalysis

ABSTRACT

The boron doped titanium oxide hybrid hollow microspheres were easily prepared by hydrothermal method. The scanning and transmission electron microscopy images demonstrated that the hybrid hollow microspheres possessed smooth outer shell and hollow interior. Their crystal structure, chemical state, amount of surface active groups and spectral response region were characterized by X-ray diffraction, X-ray photoelectron spectroscopy, infrared spectra and UV–Vis diffuse reflection spectra, respectively. Methylene blue aqueous solution served as a target pollutant to evaluate the photo-catalytic activity under simulated sunlight. It turned out a higher photo-catalytic activity of boron doped hybrid hollow microspheres, comparing with the undoped ones.

1. Introduction

Since the photo-electro-chemical splitting of water using titanium dioxide (TiO_2) electrodes was reported in 1972 [1], large amounts of efforts have been put in developing high active photo-catalytic materials in the past three decades [2–6]. TiO_2 is one of the most important semiconductor materials, widely used in environment purification, photoelectric conversion solar cells and gas sensing [7–9]. Due to its band gap of 3.2 eV, TiO_2 shows catalytic activity only under ultraviolet light. As a consequence, it fails to use visible light accounting for near 49% of sunlight spectrum [10]. Thus, many chemists and material scientists pay much attention to extending spectral response in the visible region, and improving the photo-catalytic efficiency of TiO_2 as well. Doping metals or non-metal element, such as Ag, Fe, N, S and B, into TiO_2 is an effective method to get the red shift of absorption band of photo-catalyst [11–13]. Besides, many natural materials, e.g. TiO_2, usually show fascinating property resulting from their unique structure [14–16]. Recently, potential applications of hollow nanomaterials, especially hollow spheres, have been explored in the optical, electronic, magnetic, catalytic, bio-medicine. Compared with general core/shell nanostructures, they stand out with special internal cavity, high surface area and low density [17–19]. There are several routes on the synthesis of hollow spheres, such as template method, chemically induced self-transformation route [20] and Ostwald ripening approach [11]. Specifically, templates include hard template using polyethylene spheres [21] or silica spheres [22] as scarified reagent and soft template using surfactant [23] or ionic liquid [24] as scarified template.

In our previous works [25,26], the hydrothermal route was successfully applied in preparation of Fe-doped, N-doped, (Fe, N)-codoped and undoped TiO_2, and the sol-gel auto-ignition route in N-doped TiO_2. The N-doped TiO_2 resulted in better photo-catalytic activity. However, some others [27–29] found that boron doping TiO_2 could get a higher photo-catalytic performance, while the absorption edge of photo-catalyst shifted towards the longer wavelength region. Up to now, there are few publications about the B modified TiO_2 hollow microspheres, but without reference of their microstructure changes. Zaleska et al. [30] argued that the formation of Ti–O–B species in TiO_2 powders was responsible for its higher photo-activity. In this work, we focused on a new and facile hydrothermal synthesis of B-doped TiO_2 hybrid hollow microspheres, using glucose, $(NH_4)_2TiF_6$ and H_3BO_3 as raw materials. The photo-catalytic activity was evaluated by decolorization of MB, for the samples with and without doping boron. In particular, the microstructure of as-prepared hollow spheres is tunable and their photo-catalytic activity varies with the B doping.

* Corresponding authors at: Department of Chemical Engineering, Sichuan University, 24, South Section 1, Yihuan Road, Sichuan, Chengdu 610065, China.
Tel.: +86 28 85403836; +86 28 85461108.
E-mail addresses: 301zql@vip.sina.com (Z. Liu), chuwei1965@scu.edu.cn, chuweil1965_SCU@yahoo.com (W. Chu).

0925-8388/$ – see front matter © 2010 Elsevier B.V. All rights reserved.
doi:10.1016/j.jallcom.2010.12.152

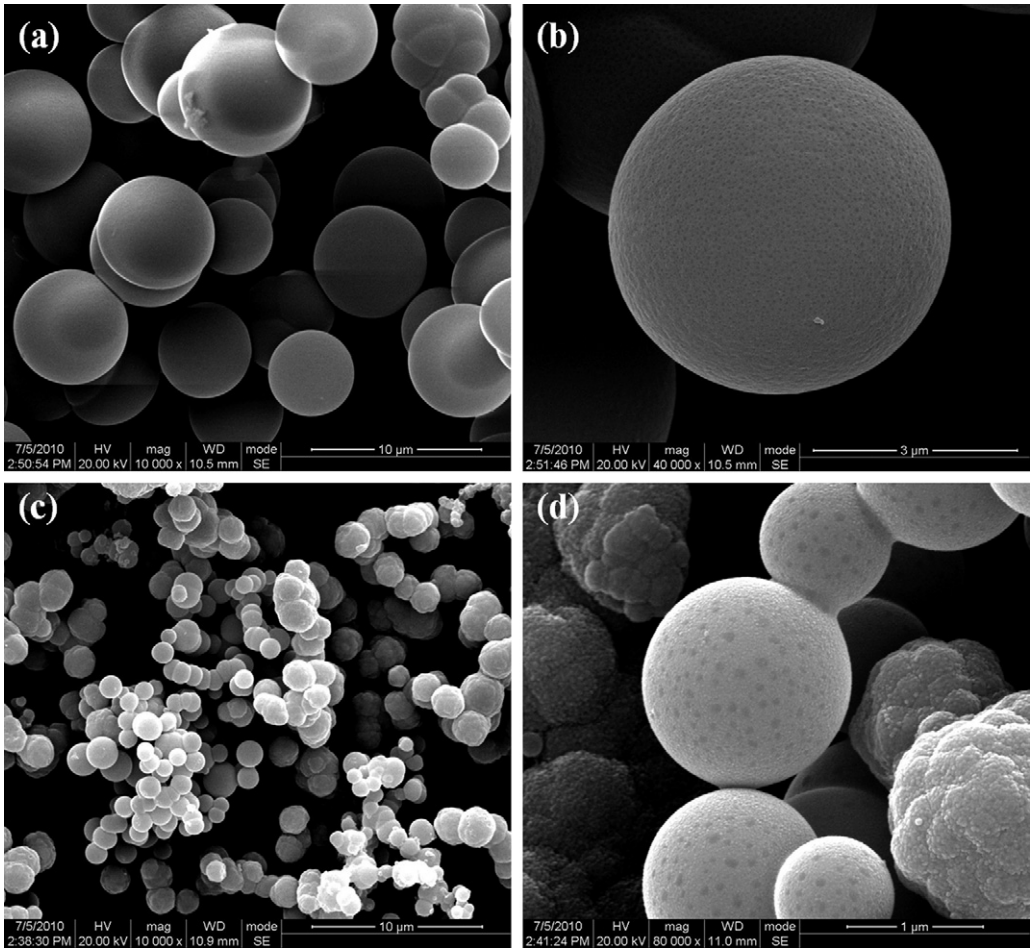

Fig. 1. FE-SEM images of the B-doped titanium oxide microspheres. (a) before calcination (×10,000), (b) before calcination (×40,000), (c) after calcination (×10,000), and (d) after calcination (×80,000).

2. Experimental

2.1. Sample preparation

The B-doped TiO_2 hybrid oxide was synthesized by one-pot hydrothermal method as that in Li's report [31]. $(NH_4)_2TiF_6$, H_3BO_3 and glucose were utilized as titanium source, boron source and template, respectively. Under intensive stir condition, a clear solution was obtained from a mixture with ratios as follows: 35 ml distilled water with 7.5 g glucose, 10 ml distilled water with 0.092 g H_3BO_3 and 20 ml distilled water with 1.5 g $(NH_4)_2TiF_6$. Then, the mixture was transferred into a Teflon-lined stainless steel autoclave and operated by hydrothermal treatment at 180 °C for 10 h. After the reaction, products were prepared through a series of operations: cooling (room temperature), filtration, washing (with de-ionized water and absolute ethanol), drying (at 80 °C for 10 h), calcining (at 500 °C for 4 h). For comparison, pure TiO_2 hollow spheres were also prepared by the same method only without the addition of H_3BO_3.

2.2. Characterizations of the hollow microspheres

Various measuring instruments were involved in describing the as-synthesized hollow microspheres. For example, FE-SEM (Inspect, FEI Corporation) and TEM (Tecnai G2 F20 S-Twin) were used for their morphologies. XRD measurement was for the structure and phase purity on a Philips X'pert PRO diffractometer using Cu Kα radiation ($\lambda = 0.15406$ nm), with an accelerating voltage of 40 kV and tube current 40 mA. In addition, XPS was conducted with a VG ESCALAB Mk II spectrometer with Al Kα radiation (1486.6 eV). The charging effects were corrected with reference to the C 1s value of the adventitious carbon (284.6 eV). IR spectra were performed at room temperature on a Bruker Tensor 27 FTIR spectrometer with KBr pellets, which was at a resolution of 4 cm^{-1} and 16 scans. UV–Vis DRS were recorded on a Hitachi U-3010 spectrophotometer with an integrating sphere attachment, in the wavelength range of 200–700 nm. $BaSO_4$ was used as a reference.

2.3. Evaluation of photo-catalytic activity

Photo-catalytic activity of the samples was evaluated by decolorization of aqueous solution of methylene blue (MB) in a 250 ml quartz reactor. A 300 W Xenon-lamp was used to simulate the sunlight spectrum. Meanwhile, 200 ml MB solution with an initial concentration of 10 mg l^{-1} was mixed with 50 mg catalyst under stir. In order to establish MB adsorption–desorption equilibrium before the reaction, the mixture was stirred using a magnetic stir-bar in the dark for 2 h. The MB solution was kept with distance of 20 cm from the Xenon-lamp. During the reaction, the temperature was controlled at 30 ± 2 °C through continuously cooling the reactor with a fan. At the same time, air was bubbled into the reactor. The MB concentration was timely determined through taking a sample every 10 min. These samples were firstly centrifuged at 4000 rpm for 10 min, finally measures using a V-5000 spectrophotometer at 660 nm. For comparison, the commercialized Degussa P25 was also used for decoloration of MB solution.

3. Results and discussion

3.1. Electron microscope images

Fig. 1 shows the typical FE-SEM images of B-doped microspheres before and after calcination. The microspheres have a diameter ranging from 3 to 6 μm and a smooth surface before calcination (see Fig. 1a and b). A distinct shrinkage is observed when the core carbon of microspheres are removed after calcination, with a diameter range from 0.5 to 2 μm (see Fig. 1c and d). According to the previous report [31], the hollow interior could be easily generated from the removal of numerous carbon templates during calcination. The TEM images of the B-doped microspheres are presented in Fig. 2

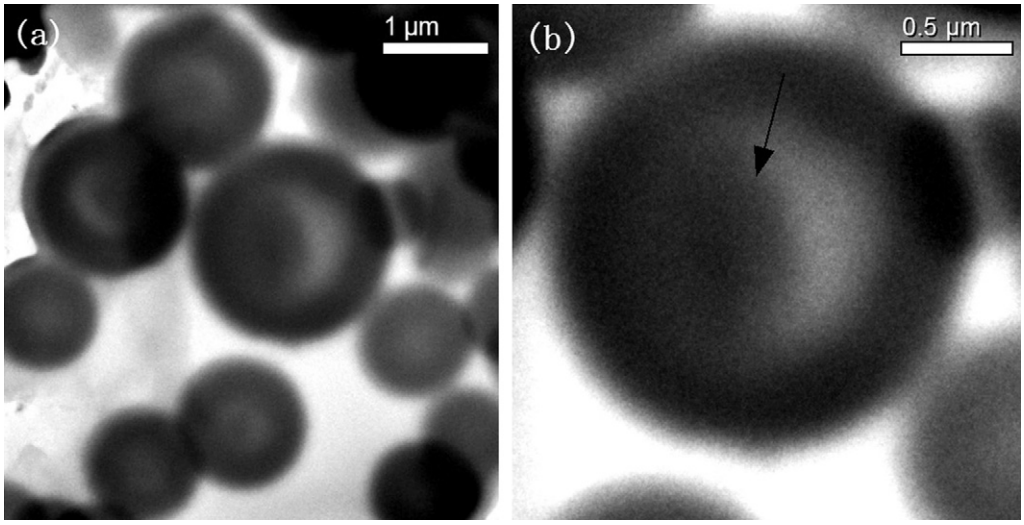

Fig. 2. (a) TEM result of the B-doped TiO_2 microspheres and (b) TEM image of one single microsphere of the sample after calcination.

for further investigation of internal structure and morphology. The obvious electron density difference between the bright centers and the dark edges confirms the existence of hollow interior [32–34]. In addition, novel double shelled hollow structures appear at the hollow microspheres. It demonstrates that the hydrothermal synthesis method using glucose as template can facilely and efficiently synthesize B-doped titanium oxide hollow microspheres. Furthermore, the sizes and the shell thickness of the microspheres would be adjusted by changing the precursor content and technological conditions [35,36].

3.2. Photo-catalytic performance of the new microspheres

Fig. 3 depicts the MB degradation rate and the apparent rate constants of various photo-catalysts under the simulated sunlight. To evaluate the photo-catalytic of the as-prepared microspheres, the degradation of methylene blue dye with the initial concentration of 10 mg l^{-1} was carried out. The experimental data were converted to observed rate constants using pseudo-first-order kinetics model [37], shown in the upper left corner of Fig. 3. It is illustrated that there is no obvious degradation under light irradiation only, without any photocatalyst. Instead, the simulative sunlight lasting for 60 min is conducive to the degradation rate, 84.1% and 72.9% for the B-doped and undoped microspheres, respectively. Evidently, the former reaction rate is much higher than the latter, but is slightly lower than that of P25. Subsequently, several characterization techniques were taken into consideration to analyze the reasons for this phenomenon.

3.3. XRD patterns of the microspheres

The powder XRD experiments of as-prepared hollow microspheres were performed to investigate the changes of TiO_2 phase structure after boron doping. The XRD patterns are presented in Fig. 4. It shows that the anatase phase is the main crystal form of TiO_2 in both the B-doped and undoped TiO_2 hollow microspheres after calcination at 500, (JCPDS 21-1272). Moreover, a certain extent of anatase has been presented in the sample before calcination. However, there were neither B_2O_3 phase nor TiB_2 phase in any of these samples. Differently, the presence of rutile can be observed in the undoped TiO_2 hollow microspheres, but failed in the B-doped sample. According to the previous report, when the atomic ratio of B to Ti was higher than 5/100, the boron would retard the anatase-

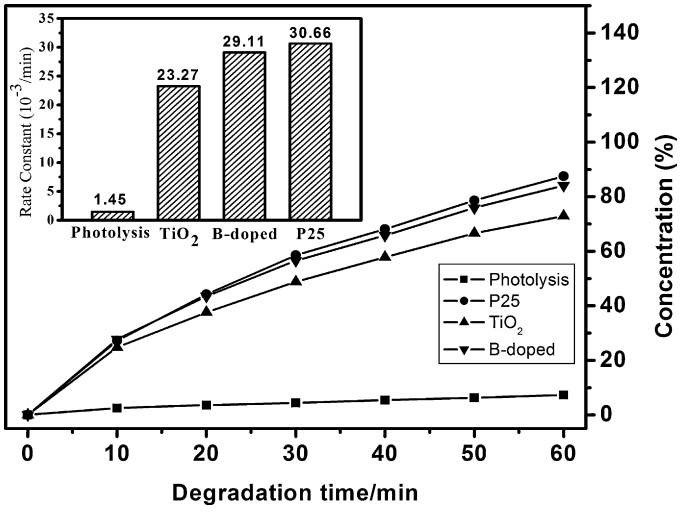

Fig. 3. Methylene blue degradation rate under visible and of various photo-catalysts. Inset: the apparent rate constants.

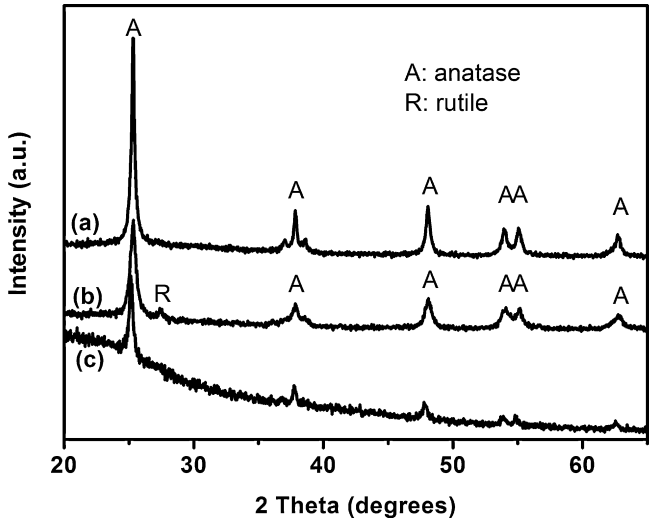

Fig. 4. XRD patterns of three prepared samples (a) B-doped TiO_2 after calcination, (b) pure TiO_2 after calcination, and (c) B-doped TiO_2 before calcination.

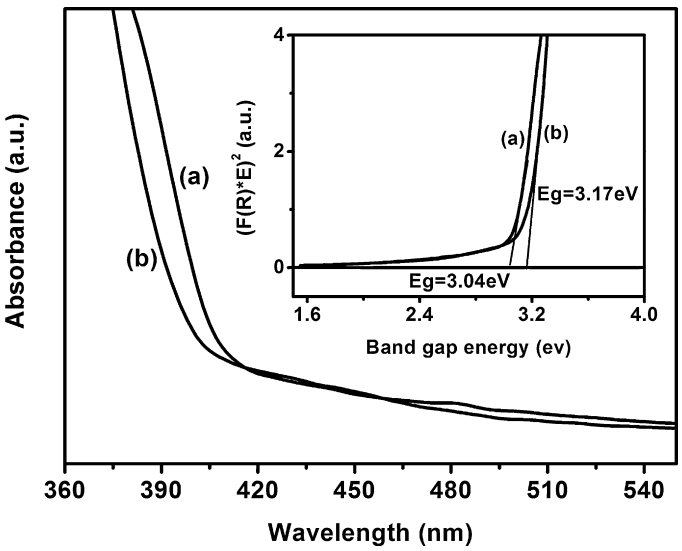

Fig. 5. UV–Vis DRS (a) B-doped microspheres and (b) undoped microspheres. Inset: Kubelka-Munk transformed reflectance spectra.

to-rutile transformation [38]. The result in this study with the atom ratio of 20/100 is in accordance with the conclusion. In addition, the diffraction peaks' intensities of B-doped microspheres are larger than those of the undoped sample, which demonstrates that the crystallinity of TiO_2 could be improved by B doping. Paulose and co-workers [39,40] reported that, as the charge–carrier recombination centers, the amorphous regions and grain boundaries of TiO_2 will be reduced as the crystallinity increases, herein the photo-catalytic performance of TiO_2 after B doping is increased.

3.4. UV–Vis DRS

Fig. 5 gives the UV–Vis DRS of prepared B-doped and undoped microspheres. As compared to undoped sample (390 nm), the spectra show the absorption edge shift to longer wavelength (408 nm) after doping B. The UV–Vis DRS can be employed to estimate the shift in the band gap transition of the photo-catalysts. Due to the Kubelka–Munk function, the band gap energy E (eV) for each specimen can be calculated by the absorption coefficient of adsorption spectra [41,42]. The Kubelka–Munk transformed reflectance spectra of B-doped and undoped microspheres are 3.04 eV and 3.17 eV, respectively. These results suggest that the B-doped microspheres would possess a better response to the visible light. Several factors determine the red-shift in B-doped sample: B atoms were incorporated into the lattice of TiO_2, partial O atoms were substituted by B atoms, the 2p orbit of B was mixed with the O 2p orbit, etc. [42,43]. What's more, the substitution of B for O leads to the photo-absorption region widened and the band gap narrowed. It will facilitate the excitation of an electron from the valence band to the conduction band and finally enhance the photo-catalytic activity of TiO_2 [44].

3.5. X-ray photoelectron spectroscopy (XPS) studies of the microspheres

The DRS results indicated the replacement of O by B in the TiO_2 lattice. Thus, it comes to the question how it changes the microstructure of TiO_2 after B doping. X-ray photoelectron spectroscopy is utilized to investigate the chemical states of the elements in the microspheres. B 1s XPS spectra of B-doped microspheres and undoped microspheres are presented in Fig. 6. A B 1s peak is shown at the nearby ca. 191 eV for the B-doped microspheres. However, there is no distinct peak for the undoped sample. The standard binging energy of B 1s in B_2O_3 and TiB_2 is 194.1 eV and 188.2 eV, respectively [42]. The results indicated that the B atom was incorporated into TiO_2 and the Ti–O–B structure was formed by its substitution of O atom [40,42,45]. Zaleska et al. [30] reported that the formation of Ti–O–B species after doping B will improve the photo-activity of TiO_2.

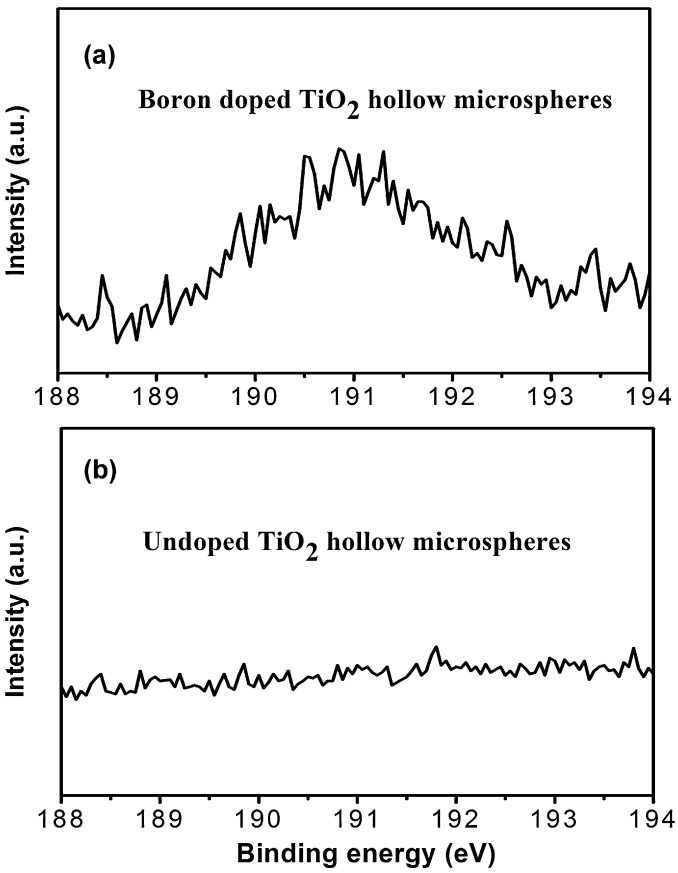

Fig. 6. B 1s high-resolution XPS spectra of (a) B-doped TiO_2 microspheres and (b) undoped TiO_2 microspheres.

The high-resolution XPS spectra of the O 1s of the samples are also shown in Fig. 7. The O 1s peaks of the undoped microspheres

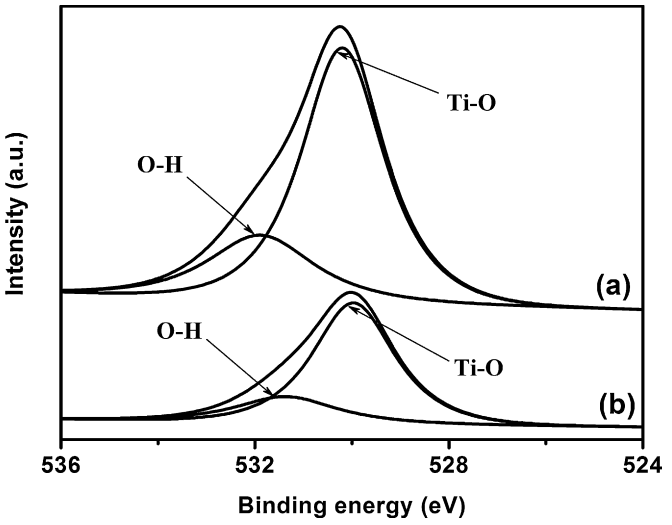

Fig. 7. O 1s high-resolution XPS spectra of (a) B-doped TiO_2 microspheres and (b) undoped TiO_2 microspheres.

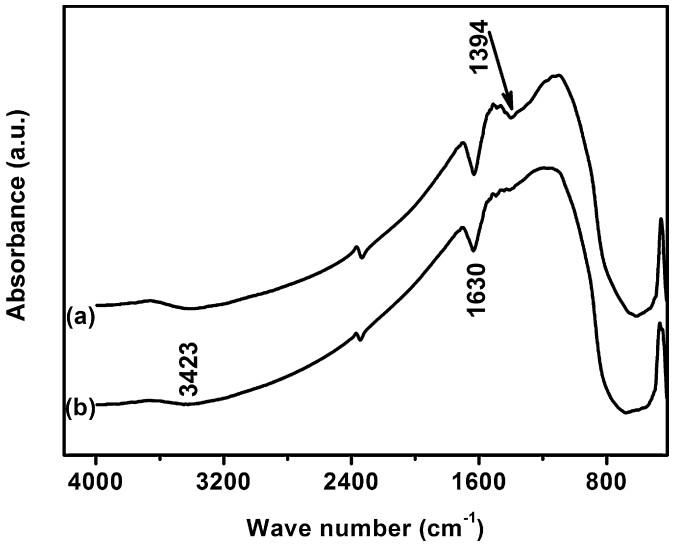

Fig. 8. FTIR spectra of (a) B-doped TiO_2 microspheres and (b) undoped TiO_2 microspheres.

at 529.9 eV and 531.4 eV are attributed to the crystal lattice oxygen (Ti–O) in TiO_2 and hydroxyl groups (O–H) on the microspheres surface, respectively [25,42]. The similar two peaks at 530.2 eV and 531.9 eV of the B-doped microspheres are also corresponding to oxygen in the Ti–O bond and O–H bond, respectively. The significant increase in binding energy of crystal lattice oxygen after the B-doped (0.5 eV) indicated that the microstructure of the microspheres has been really changed by the boron incorporation. It is well known that the hydroxyl groups on the TiO_2 surface have positive impacts on the photo-catalytic reaction [46]. In the case of the O 1s peak area, the hydroxyl group content on the surface of undoped microspheres is 20.30%, while it increases to 23.84% after the boron doping. In addition, the sum of the two kinds of oxygen species in B-doped sample is higher than that in unpoded one. As a consequence, it may also account for the enhancement of photo-catalysis efficiency resulting from the boron incorporation.

3.6. IR spectra study of the microspheres

Fig. 8 shows the IR spectra of B modified and unmodified samples in the range 4000–500 cm^{-1}. The spectra around the 650 cm^{-1}, which are assigned to the vibrations of the Ti–O bonds in the deformed octahedra of anatase titania, exhibit distinct expansion of band regions [25,47]. The bands at 3423 cm $^{-1}$ and 1630 cm^{-1} correspond to the surface adsorbed water and hydroxyl groups [31]. As to the B-doped microspheres, a distinct peak at 1394 cm^{-1} can be observed, which refers to the Ti–O–B bond [38,48]. However, this peak cannot be found for the undoped TiO_2 samples. It demonstrates that the B atoms have entered into the lattice of TiO_2 and O atoms are substituted by B atom to form the Ti–O–B structure. This is in well agreement with the result of XPS studies above.

4. Conclusions

In summary, the boron doped titanium oxide hybrid hollow microspheres with higher photo-catalytic activity under visible light have been successfully fabricated by a facile hydrothermal route. The boron addition exhibits a significant positive influence on the crystallinity, microstructure, surface hydroxyl groups and photo-catalytic performance of the TiO_2 hollow microspheres. Results showed the substitution of O atom by the incorporated boron in the lattice. The boron doping conduced to the improvement in crystallinity of anatase titania and the increase in amount of superficial hydroxyl groups. In addition, the improvement of TiO_2 hollow microspheres in the UV–Vis spectral response and photocatalytic activity can be achieved by the boron incorporation in the new microspheres. All in all, the present work provides a convenient and effective way to prepare TiO_2 hollow microsphere, which shows high photo-activity in visible region.

Acknowledgements

This work was supported by National Basic Research Program of China (973 Program, 2011CB201202) of Ministry of Science and Technology of China (MOST), National Natural Science Foundation of China (20776089 and 50774053) and the 985 Project of Sichuan University. The authors gratefully acknowledge the TEM Group of Analytical Testing Center of Sichuan University and helpful discussions from Dr. Wenjing Sun and Yali Tang.

References

[1] A. Fujishima, K. Honda, Nature 238 (1972) 37–38.
[2] S. Yanagida, K. Mizumoto, C. Pac, J. Am. Chem. Soc. 108 (1986) 647–654.
[3] M.R. Hoffmann, S.T. Martin, W.Y. Choi, D.W. Bahnemann, Chem. Rev. 95 (1995) 69–96.
[4] J.S. Hu, L.L. Ren, Y.G. Guo, H.P. Liang, A.M. Cao, L.J. Wan, C.L. Bai, Angew. Chem. Int. Ed. 44 (2005) 1269–1273.
[5] L. Djellal, S. Omeiri, A. Bouguelia, M. Trari, J. Alloys Compd. 476 (2009) 584–589.
[6] D. Li, H. Haneda, S. Hishita, N. Ohashi, Chem. Mater. 17 (2005) 2596–2602.
[7] C.H. Ao, S.C. Lee, Chem. Eng. Sci. 60 (2005) 103–109.
[8] U. Bach, D. Lupo, P. Comte, J.E. Moser, F. Weissrtel, J. Salbeck, J.H. Spreitzer, M. Gratzel, Nature 395 (1998) 583–585.
[9] D. Buso, M. Post, C. Cantalini, P. Mulvaney, A. Martucci, Adv. Funct. Mater. 18 (2008) 3843–3849.
[10] Y.A. Shaban, S.U.M. Khan, Chem. Phys. 339 (2007) 73–85.
[11] J.K. Zhou, L. Lv, J.Q. Yu, H.L. Li, P.Z. Guo, H. Sun, X.S. Zhao, J. Phys. Chem. C 112 (2008) 5316–5321.
[12] R. Asahi, T. Morikawa, T. Ohwaki, K. Aoki, Y. Taga, Science 293 (2001) 269–271.
[13] S.S. Srinivasan, J. Wade, E.K. Stefanakos, Y. Goswami, J. Alloys Compd. 424 (2006) 322–326.
[14] G.K. Mor, K. Shankar, M. PauloseM, O.K. Varghese, C.A. Grimes, Nano. Lett. 6 (2006) 2011–2075.
[15] G. Li, Z.Q. Liu, J. Lu, L. Wang, Z. Zhang, Appl. Surf. Sci. 255 (2009) 7323–7328.
[16] J. Yu, Y. Chen, J. Alloys Compd. 504 (2010) s364–s367.
[17] S.S.K. Kamal, P.K. Sahoo, M. Premkumar, N.V.R. Rao, T.J. Kumar, B. Sreedhar, A.K. Singh, S. Ram, K.C. Sekhar, J. Alloys Compd. 474 (2009) 214–218.
[18] J.G. Yu, W. Liu, H.G. Yu, Cryst. Growth Des. 8 (2008) 930–934.
[19] Y. Wang, F.B. Su, J.Y. Lee, X.S. Zhao, Chem. Mater. 18 (2006) 1347–1353.
[20] D.G. Tong, X.L. Zeng, W. Chu, D. Wang, P. Wu, J. Mater. Sci. 45 (2010) 2865–2867.
[21] S.W. Kim, M. Kim, W.Y. Lee, T. Hyeon, J. Am. Chem. Soc. 124 (2002) 7642–7643.
[22] T. He, D.R. Chen, X.L. Jiao, Y.Y. Xu, Y.X. Gu, Langmuir 20 (2004) 8404–8408.
[23] T. Nakashima, N. Kimizuka, J. Am. Chem. Soc. 125 (2003) 6386–6387.
[24] J.G. Yu, H.T. Guo, S.A. Davis, S. Mann, Adv. Funct. Mater. 16 (2006) 2035–2041.
[25] Z.Q. Liu, Y.C. Wang, W. Chu, Z.H. Li, C.C. Ge, J. Alloys Compd. 501 (2010) 54–59.
[26] Z.Q. Liu, Y.P. Zhou, Z.H. Li, Y.C. Wang, C.C. Ge, Rare Met. 26 (2007) 263–270.
[27] Y. Huang, W.K. Ho, Z.H. Ai, X. Song, L.Z. Zhang, S.C. Lee, Appl. Catal. B: Environ. 89 (2009) 398–405.
[28] N. Lu, H.M. Zhao, J.Y. Li, X. Quan, S. Chen, Sep. Purif. Technol. 62 (2008) 668–673.
[29] R. Khan, S.W. Kim, T.J. Kim, C.M. Nam, Mater. Chem. Phys. 112 (2008) 167–172.
[30] A. Zaleska, J.W. Sobczak, E. Grabowska, J. Hupka, Appl. Catal. B: Environ. 78 (2008) 92–100.
[31] G. Li, F. Liu, Z. Zhang, J. Alloys Compd. 493 (2010) L1–L7.
[32] B.X. Li, Y. Xie, M. Jing, G.X. Rong, Y.C. Tang, G.Z. Zhang, Langmuir 22 (2006) 9380–9385.
[33] L.P. Zhu, H.M. Xiao, W.D. Zhang, G. Yang, S.Y. Fu, Cryst. Growth Des. 8 (2008) 957–963.
[34] H. Peng, L.J. Yu, A.H. Zuo, C.Y. Guo, F.L. Yuan, J. Phys. Chem. C 113 (2009) 900–906.
[35] Y.Z. Li, T. Kunitake, S. Fujikawa, J. Phys. Chem. B 26 (2006) 13000–13004.
[36] Y.W. Zhang, M. Jiang, J.X. Zhao, J. Zhou, D.Y. Chen, Macromolecules 37 (2004) 1537–1543.
[37] J.J. Wu, X.J. Lü, L.L. Zhang, Y.J. Xia, F.Q. Huang, F.F. Xu, J. Alloys Compd. 496 (2010) 234–240.
[38] D.M. Chen, D. Yang, Q. Wang, Z.Y. Jiang, Ind. Eng. Chem. Res. 45 (2006) 4110–4116.
[39] M. Paulose, G.K. Mor, O.K. Varghese, K. Shankar, C.A. Grimes, J. Photochem. Photobiol. A: Chem. 178 (2006) 8–15.

[40] J.Y. Li, N. Lu, X. Quan, S. Chen, H.M. Zhao, Ind. Eng. Chem. Res. 47 (2008) 3804–3808.
[41] A.E. Morales, E.S. Mora, U. Pal, Rev. Mex. Fis. 53 (2007) 18–22.
[42] W. Zhao, W.H. Ma, C.C. Chen, J.C. Zhao, Z.G. Shuai, J. Am. Chem. Soc. 126 (2004) 4782–4783.
[43] H. Geng, S.W. Yin, X. Yang, Z.G. Shuai, B.G. Liu, J. Phys.: Condens. Matter. 18 (2006) 87–96.
[44] Y.L. Su, S. Han, X.W. Zhang, X.Q. Chen, L.C. Lei, Mater. Chem. Phys. 110 (2008) 239–246.
[45] J.J. Xu, Y.H. Ao, M.D. Chen, D.G. Fu, J. Alloys Compd. 484 (2009) 73–79.
[46] A. Fujishima, X.T. Zhang, D.A. Tryk, Surf. Sci. Rep. 63 (2008) 515–582.
[47] G.M. Krishna, N. Veeraiah, N. Venkatramaiah, R. Venkatesan, J. Alloys Compd. 450 (2008) 477–485.
[48] K.Y. Jung, S.B. Park, S.K. Ihm, Appl. Catal. B: Environ. 51 (2004) 239–245.